VERSITA

OPTO-ELECTRONICS REVIEW **14**(4), 263–267

DOI: 10.2478/s11772-006-0034-9

Observation of out-coupling of a nematicon

J. BEECKMAN*[1], K. NEYTS[1], X. HUTSEBAUT[2], and M. HAELTERMAN[2]

[1]Liquid Crystals & Photonics Group, Department of Electronics and Information Systems, Ghent University, Sint-Pietersnieuwstraat 41, 9000 Gent, Belgium

[2]Service d'Optique et Acoustique, Université libre de Bruxelles CP 194/5, 50 Roosevelt Ave., 1050 Bruxelles, Belgium

In this work we present the observation of spatial optical solitons in liquid crystal cells by recording the diffraction pattern of the out-coupled beam on a distant screen. Simultaneously, the light propagation is observed via scattering measurements. The most important observation is displacement of the beam on the screen due to the transverse undulation inside the cell. This undulation is caused by the anisotropic walk-off of the beam. The displacement is in good agreement with the values of the undulation earlier reported.

Keywords: liquid crystals, optical spatial solitons, lateral light propagation.

1. Introduction

Nematicons [1] are spatial optical solitons [2] in nematic liquid crystals. They have been generated in these materials by either thermal nonlinearities [3] or reorientational nonlinearities [4–6]. Due to the molecular reorientation under the influence of a linearly polarized optical electric field, the refractive index is higher where the optical intensity is higher. This leads to a focusing non linear effect that can compensate for the spreading of the beam occurring during propagation because of natural diffraction [7]. In this way, it becomes possible to propagate beams with practically invariant intensity profile, these entities are called spatial solitons and nematicons if we are dealing with nematic liquid crystals. During the last five years, the applicability of these nematicons in all-optical switching and optical reconfigurable interconnects has been demonstrated. It is namely possible to steer the beam by means of soliton interactions [8] or by means of patterned electrodes [9]. Easy fiber-to-fiber interconnection is possible by soliton merging [10]. An effect that has been recently demonstrated numerically and experimentally is the transverse undulation of the nematicon for certain configurations [11,12]. The undulation of the beam inside the cell is caused by an off-axis deviation of the beam, due to the optical anisotropy that appears when the liquid crystal molecules reorient. Because of this off-axis deviation, the path of the beam shows a periodic undulation and this undulation is nearly sinusoidal for low voltages.

To the best of our knowledge, in all the reported experiments on nonlinear waveguiding in liquid crystals, the beam propagation in the cell is observed either via the light scattered by the liquid crystal [4–10] or via indirect observation by visualization of the self-induced waveguide [7,13]. In these measurements, the light beam (or the material properties) can only be observed in the plane parallel to the glass surfaces, while no information is available along the thickness of the cell. Via some tricks, it is possible to get some information along this direction, for example by tilting the camera such that the cell is viewed from an angle of 45° [11] or by using capillary cells [14] (i.e., cylindrical cells with an inner diameter of a few micrometer). These methods, however, cannot give detailed information about the actual beam characteristics. Indeed, since the measurements are based on scattering the observed intensity is always an integration of the scattered light along the viewing direction.

In the present work, we overcome these difficulties by making cells that allowed the out-coupling of the beam, namely with an entrance and an exit window for the light. In this way we are able to look at the beam itself at the output of the cell in order to gather some information about the behaviour of the beam along the thickness of the cell. Since the beam power reduces significantly along the propagation distance [7], the length of the cell along the propagation distance has to be small enough, in the order of a few millimetres. The cutting of narrow glass plates is done with a diamond saw, because the glass facets should be very smooth. The glass plates in this cell are 15×4×1.1 mm and are glued together with spacers in between, in order to assure a homogeneous thickness of 75 μm as shown in Fig. 1(a). The glass plates are treated with an alignment layer and the rubbing is along the z direction as denoted in Fig. 1(a). The glass plates have also been coated with ITO electrodes in order to apply the voltage V across the cell to overcome the Frederiks threshold [5]. In the absence of

*e-mail: jeroen.beeckman@elis.ugent.be

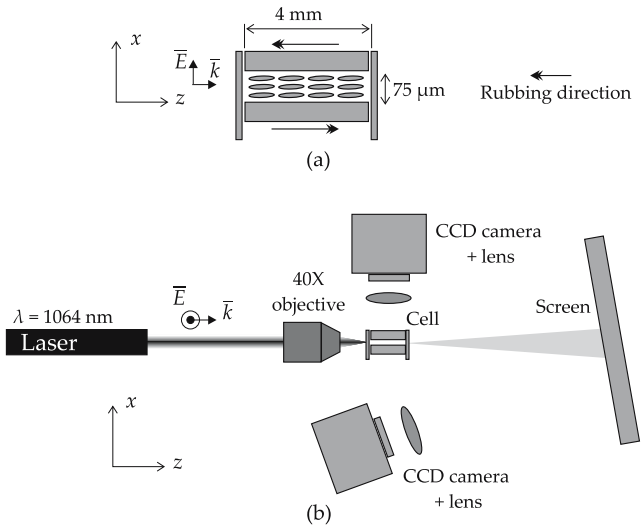

Fig. 1. Scheme of the set-up to measure the outgoing of the beam. The diffraction pattern is observed on a distant screen with a second CCD camera.

electrical and optical fields, the director orientation should be uniform inside the cell, with a pretilt angle of 2°. Two additional thin glass plates (entrance and exit window) are mounted perpendicularly at the facets of these thick glass plates. The cell is then filled with the nematic liquid crystal E7 by Merck n_o =1.5038 and n_e = 1.6954 at λ = 1064 nm.

The set-up used for the measurements is depicted in Fig. 1(b). A CW laser beam from a Nd:YAG laser λ = 1064 nm is injected inside the cell by means of a 40X objective lens. Two CCD cameras are used simultaneously, namely one camera for the regular scattering measurements and one camera for the observation of the diffraction pattern on the screen. The beam coming out of the cell can freely diffract on the screen and the intensity pattern is observed with the second camera. This camera is equipped with a standard camera lens. The screen is placed at a distance of approximately 6.5 cm from the exit of the cell. The angle of the screen and the CCD chip with respect to the output window of the cell is made as small as possible to reduce distortions in recording the diffracted pattern.

2. Diffraction patterns

Figure 2 shows the diffracted patterns for different voltages and different optical powers. In order to understand these patterns, one should recall that the angle of the far-field divergence θ_{ffd} of a Gaussian beam obeys $\tan\theta_{ffd} = 2/k_0 w_0$ [15], where k_0 is the wavenumber in vacuum and w_0 is the waist of the Gaussian beam. For a Gaussian beam with a waist of 3 μm, the value of $\tan\theta_{ffd}$ is 0.113. Suppose that the beam inside the cell is a pure soliton, then the waist of the beam at the output of the cell should be the same. For a screen distance of 6.5 cm, this results in a full width of the intensity pattern of about 1 cm. Note that the waists of amplitude and intensity distributions relate to each other as the square root of 2. Suppose that the beam diffracts inside the cell, then this calculation is correct, but the screen distance should be the sum of 6.5 cm and the optical path length due to the cell length, which in this case is a distance of about 6.5 cm + 4 mm. This means that the width of the intensity pattern on the screen changes by roughly $\tan\theta_{ffd}$×4 mm, which is less than 1 mm and hardly observable with the set-up.

If we look at the upper patterns in Fig. 2, then we see that the width of the intensity pattern is practically unchanged. The width of the intensity pattern corresponds well with the value of 1 cm that was expected.

The patterns that we observe in Fig. 2 are not the smoothly varying Gaussian profiles that we expect, but exhibit flecks or speckle. The origin should be related to the propagation in the cell or the transmission through the entrance or exit region. It can actually be caused by a number of effects: dirty entrance or exit window, small-scale variations in director orientation, multi-mode properties of the waveguide or impurities in the liquid crystal. The fact that the fleck effect increases with increasing voltage, might point to the fact that there is a disclination present in the cell. The observation of light propagation by scattering, however, does not reveal any disclination. Another possibility is that with increasing voltage, the scattered light along the propagation distance mixes with the original beam. This effect increases with increasing voltage since the scattered light cannot exit the liquid crystal layer easily at higher voltages because of the higher index contrast between the centre of the liquid crystal layer and the liquid crystal near the edges.

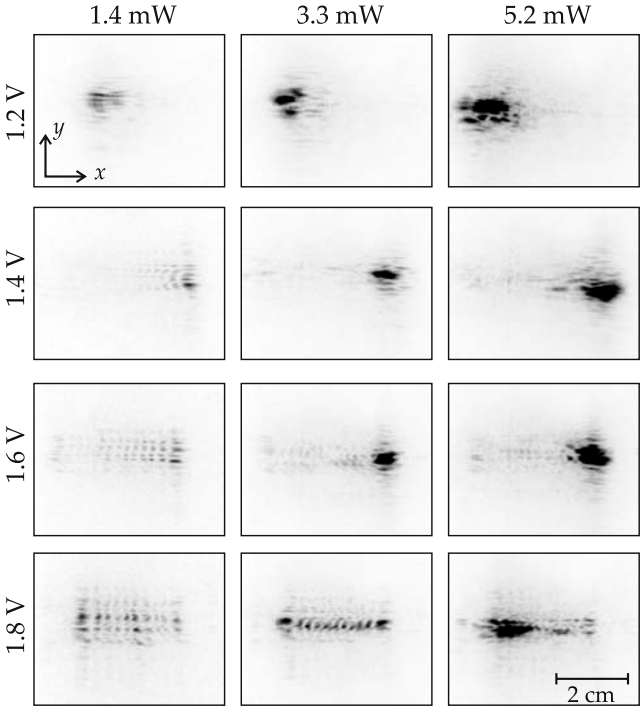

Fig. 2. Images of the diffraction pattern on the screen for different voltages across the cell and optical power.

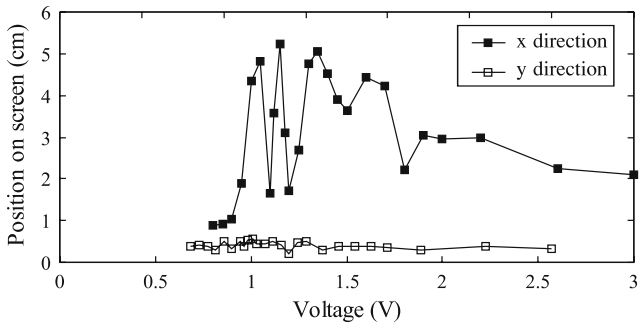

Fig. 3. The measured position of the beam on the external screen, $\hat{x}$ and $\hat{y}$ in function of voltage.

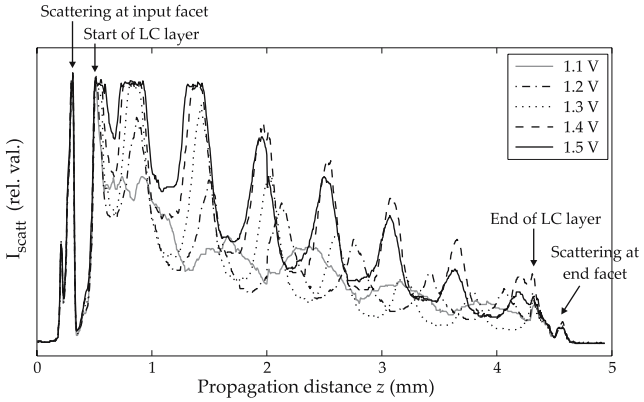

Fig. 4. Evolution of the maximum of the recorded beam from the scattering measurement I_{scatt} along the propagation distance z.

3. Beam position on the screen

The x and y coordinates of the centre of mass of the diffracted beam on the screen ($\hat{x}$ and $\hat{y}$) are numerically extracted for each diffraction pattern. The resulting positions for different voltages are plotted in Fig. 4. The $\hat{y}$ position is approximately constant. The $\hat{x}$ position changes drastically with voltage. The amplitude of this variation is in the range of 3 to 4 cm. If we assume that the direction of energy flow in the cell makes a maximum angle of 7° with respect to the z axis [11], then from Snell's law we know that the angle in air of the beam is ranging from zero to 21°. The value of 3 to 4 cm corresponds to a maximum angle in air of 24.8° to 31.6°, which is somewhat larger than the 21° that was expected.

4. Scattered intensity oscillation

Figure 4 shows the maximum intensity of scattered light of the soliton beam in function of the propagation distance for different voltages. This means that for each z the maximum of the scattered intensity over the y coordinate is entered in the graph and this value is called I_{scatt}. After careful analysis of the recorded pictures it was concluded that the first and the last peak in the graph are originating from scattering from the input and output window of the cell. These peaks will not be considered for the further analysis. The graph shows that for some voltages the peaks are more pronounced than others. The period of the intensity modulation also changes with voltage. To analyze this effect, the z positions of the maxima in I_{scatt}, or z_{max}, are plotted in Fig. 5 as a function of the applied voltages.

From the z_{max} values, the average distance between two maxima Δz_{max} can be calculated. This value Δz_{max} reaches a minimum of 560 μm for a voltage of 1.45 V. For higher and lower voltages, the value increases. When comparing these values with the period of transverse undulation of the nematicon as described in Refs. 11 and 16, the correspondence is striking. This gives an indication that the periodic oscillation in beam intensity is caused by the undulative behaviour inside the cell.

With the data in Fig. 5, a cosine function can be constructed for each voltage V with the period equal to the distance between the maxima Δz_{max} and with the maxima of the cosine function correlated to the positions of the maxima Δz_{max}, as in the following equation

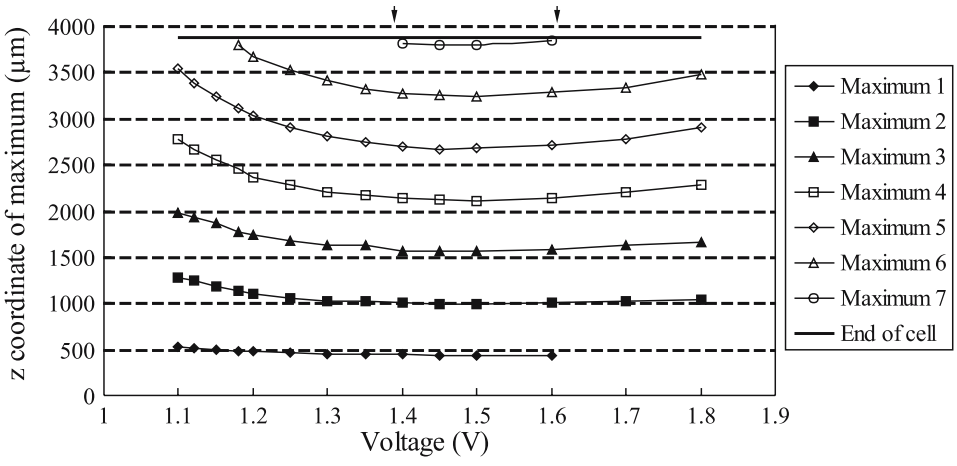

Fig. 5. The z position of the maxima z_{max} along the propagation distance versus voltage for a 75-μm-thick cell. The horizontal line denotes the end of the LC layer as estimated from Fig. 4.

$$I_{scatt}(z,V) \sim \cos\left(\frac{2\pi}{\Delta z_{\max}(V)}(z - z_{\max}(V))\right). \qquad (1)$$

The effect of the attenuation of the beam is not taken into account. If the periodic intensity modulation is indeed caused by the transverse undulation, then the derivative of this cosine function at the end of the LC layer (for $z = z_{end}$) should be related to a position of the maximum on the screen $\hat{x}$.

$$\hat{x}(V) \sim \left[\frac{d}{dz}\cos\left(\frac{2\pi}{\Delta z_{\max}(V)}(z - z_{\max}(V)) + \Phi\right)\right]_{z=z_{end}} . \qquad (2)$$

A least squares method was used to fit the derivative with the positions on the screen. The result is shown in Fig. 6. The graph shows that the data from the screen relate very well with the data of the scattering measurements. This undeniably proves that the intensity oscillations of the observed soliton beam are due to the undulation in the cell. The question that remains is at which place in the beam propagation the observed scattering intensity is maximum. To answer this, it has to be mentioned that the constant phase factor Φ has to be added to the cosine function in order to obtain the good agreement in Fig. 6. The phase factor to be added is –60°, obtained via the least squares method. Note that the minimum undulation period at 1.5 V corresponds to a turning point in Fig. 6, because

$$\left.\frac{d\Delta z_{\max}}{dV}\right|_{V\approx 1.5V} \approx 0. \qquad (3)$$

If one looks at the positions of the maxima in Fig. 5, then one can see that the maximum corresponds to the end of the cell for a voltage slightly lower than 1.4 V and for a voltage slightly higher than 1.6 V (as indicated by the arrows). In Fig. 3, one can see that for these voltages the x position of the diffracted beam is maximal. The large x values correspond to the side where the CCD camera for the scattering measurements is placed. This means that the maximum recorded scattered intensity corresponds roughly to the place where the direction of the propagation points

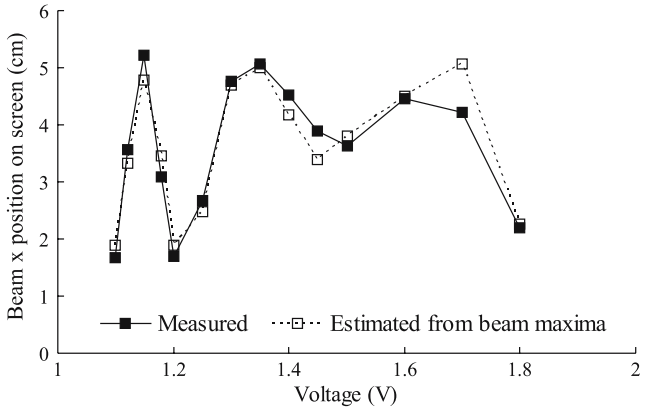

Fig. 6. Correlation between the x position of the beam on the screen $\hat{x}$ and the derivative of the cosine function of Eq. (2).

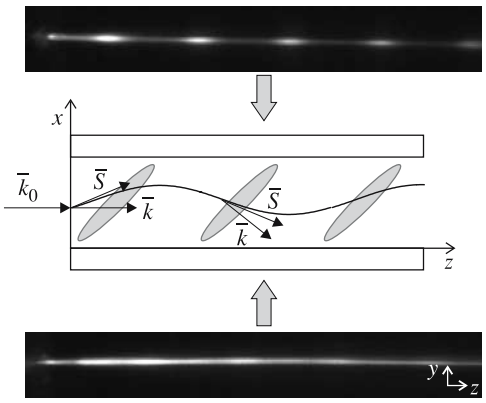

Fig. 7. Difference observed in the scattered intensity depending on which side of the cell the CCD camera is placed. The figure describes schematically the origin of this difference.

towards the CCD camera. The correspondence would be exact if the phase factor would be –90° instead of –60°. The rough estimation of the end of the LC layer z_{end} is probably the cause of this mismatch.

The fact that a higher scattered intensity is observed when the beam is propagating slightly towards the camera and a lower one is observed when the beam is propagating slightly away from the camera is quite acceptable. Indeed, in Refs. 17 and 18, it is stated that the scattering of a beam is larger for small deviation angles between the incoming and scattered beams.

There is one issue unsolved. The periodic modulation of the scattered intensity in some cells is large while in others it is hardly noticeable. The explanation of this question is that it depends on which side of the cell the CCD camera is placed. Figure 7 shows the observed intensity when looking from the top (from the positive x direction) or from the bottom (from the negative x direction). The difference is clearly visible.

This might be surprising because the cell looks symmetric and because the simulation results show that the undulation is also symmetric [11,16]. But, in fact, there is an asymmetry in the cell, which is explained in Fig. 7. The averaged Poynting vector $\overline{S}$ lies along the z axis, but the wave vector $\overline{k}$ is on average directed towards the negative x direction. On average, when looking from the bottom in Fig. 7, one can expect larger scattered intensity than when looking from the top.

5. Conclusions

In this work we present measurements of the far-field diffraction pattern of a nematicon. The measurements reveal a change in position along the direction perpendicular to the glass surfaces. This change in position is related to the periodic modulation of scattered intensity along the propagation direction. Both effects are caused by the transverse undulation of the beam. The quantitative analysis of the observed phenomena is in perfect agreement with earlier published results.

Aknowledgements

Jeroen Beeckman is Research Assistant of the Research Foundation – Flanders (FWO – Vlaanderen). Xavier Hutsebaut is funded by the Fonds pour la Formation à la Recherche dans l'Industrie et l'Agriculture (FRIA). The research is a result of collaboration within the framework of the Interuniversity Attraction Poles Program PhotonNetwork of the Belgian Science Policy. The authors would also like to thank Per Rudquist and Koen d'Havé of Chalmers University (Sweden) for the preparation of the glass plates.

References

1. G. Assanto, M. Peccianti, and C. Conti, "Nematicons: Optical spatial solitons in nematic liquid crystals", *Opt. Photon. News* **14**, 44–48 (2003).
2. M. Segev, "Optical spatial solitons", *Opt. Quant. Electron.* **30**, 503–533 (1998).
3. F. Derrien, J. Henninot, M. Warenghem, and G. Abbate, "A thermal (2D + 1) spatial optical soliton in a dye doped liquid crystal", *J. Opt. A: Pure Appl. Opt.* **2**, 332–337 (2000).
4. J. Beeckman, K. Neyts, X. Hutsebaut, C. Cambournac, and M. Haelterman, "Simulations and experiments on self-focusing conditions in nematic liquid-crystal planar cells", *Opt. Express* **12**, 1011–1018 (2004).
5. M. Peccianti, A. De Rossi, G. Assanto, A. De Luca, C. Umeton, and I. Khoo, "Electrically assisted self-confinement and waveguiding in planar nematic liquid crystal cells", *Appl. Phys. Lett.* **77**, 79 (2000).
6. M. Karpierz, M. Sierakowski, M. Swillo, and T. Wolinsky, "Selffocusing in liquid crystalline waveguides", *Mol. Cryst. Liq. Cryst.* **320**, 157–163 (1998).
7. X. Hutsebaut, C. Cambournac, M. Haelterman, J. Beeckman, and K. Neyts, "Measurement of the self-induced waveguide of a solitonlike optical beam in a nematic liquid crystal", *J. Opt. Soc. Am.* **B22**, 1424–1431 (2005).
8. M. Peccianti, C. Conti, A. Assanto, A. De Luca, and C. Umeton, "All-optical switching and logic gating with spatial solitons in liquid crystals", *Appl. Phys. Lett.* **81**, 3335–3337 (2002).
9. J. Beeckman, K. Neyts, and M. Haelterman, "Patterned electrode steering of nematicons", *J. Opt. A: Pure Appl. Opt.* **8**, 214–220 (2006).
10. J. Henninot, M. Debailleul, R. Asquini, A. d'Alessandro, and M. Warenghem, "Self-waveguiding in an isotropic channel induced in dye doped nematic liquid crystal and a bent self-waveguide", *J. Opt. A: Pure Appl. Opt.* **6**, 315–323 (2004).
11. M. Peccianti, A. Fratalocchi, and G. Assanto, "Transverse dynamics of nematicons", *Opt. Express* **12**, 6524–6529 (2004).
12. J. Beeckman, K. Neyts, X. Hutsebaut, C. Cambournac, and M. Haelterman, "Simulation of 2D lateral light propagation in nematic liquid-crystal cells with tilted molecules and nonlinear reorientational effect", *Opt. Quant. Electron.* **37**, 95–106 (2005).
13. M. Warenghem, J.F. Blach, and J.F. Henninot, "Measuring and monitoring optically induced thermal or reorientational non-locality in nematic liquid crystal", *11th Int. Topical Meeting on Optics of Liquid Crystals*, Florida, 140 (2005).
14. M. Warenghem, J. Henninot, and G. Abbate, "Non linearly induced self waveguiding structure in dye doped nematic liquid crystals confined in capillaries", *Opt. Express* **2**, 483–490 (1998).
15. K. Iizuka, *Elements of Photonics*, Wiley-Interscience, New York, 2002.
16. J. Beeckman, K. Neyts, X. Hutsebaut, C. Cambournac, and M. Haelterman, "3D simulation method for light propagation in liquid crystal structures with specific anisotropy", *Proc. 13th Int. Workshop on Optical Waveguide Theory and Numerical Modelling*, 2005.
17. P.G. De Gennes and J. Prost, *The Physics of Liquid Crystals*, International Series of Monographs on Physics, Oxford University Press, Oxford, 1995.
18. I. Khoo, *Liquid Crystals: Physical Properties and Nonlinear Optical Phenomena*, Wiley-Interscience, New York, 1994.